Available online at www.sciencedirect.com
SCIENCE DIRECT
Journal of Electroanalytical Chemistry 589 (2006) 249–258
Journal of Electroanalytical Chemistry
www.elsevier.com/locate/jelechem

Micro-cylinder biosensors for phenol and catechol based on layer-by-layer immobilization of tyrosinase on latex particles: Theory and experiment

P. Rijiravanich [a], K. Aoki [b], J. Chen [b], W. Surareungchai [a,*], M. Somasundrum [c,*]

[a] School of Bioresources, King Mongkut's University of Technology Thonburi, Bangkhuntien-Chaitalay Road, Thakam, Bangkok 10150, Thailand
[b] Department of Applied Physics, University of Fukui, 3-9-1, Bunkyo, Fukui-shi, 910-8507, Japan
[c] PDTI, King Mongkut's University of Technology, Thonburi, Bangkhuntien-Chaitalay Road, Thakam, Bangkok 10150, Thailand

Received 23 December 2005; received in revised form 7 February 2006; accepted 16 February 2006
Available online 31 March 2006

Abstract

Microelectrode sensors for phenol and catechol are described, based on the sequential immobilization of polystyrene sulphonate, polyallylamine, tyrosinase and polyallylamine again, onto micrometer scale latex spheres, followed by the adsorption of the spheres onto electrochemically pretreated carbon fibres. The steady state responses of the fibres are analyzed in terms of a cylindrical diffusion – kinetic model. It is deduced that the adsorbed latex particles provide a relatively open film structure, resulting in a diffusion coefficient only one order of magnitude lower than the solution value, and that at minimum 2–3% of the immobilized enzyme is catalytically active. The optimised sensors exhibit linear ranges to phenol and catechol of 7–56.5 μM and 2–19.7 μM respectively, with sensitivities of 0.15 A M^{-1} cm^{-2} and 1.72 A M^{-1} cm^{-2} respectively. The limiting factor to sensor stability is desorption of latex from the fibres.

Keywords: Microelectrode; Carbon fibre; Polyphenol oxidase; Mathematical model

1. Introduction

In research on enzyme immobilization, much attention has recently been focused on the layer-by-layer (LbL) self-assembly process [1–13,15]. Interest in this method stems from the fact that it is both a simple technique which may be applied to a wide range of enzymes, and that it is one of the few immobilization procedures which allows control over the amount and spatial distribution of the enzyme. The latter factor is relevant to the construction of biosensors, as the deposition of controlled amounts of enzyme in uniform films is important both for modeling studies of biosensors and for their practical application.

The principle of the LbL process, as first introduced by Decher and Hong [1], is that a surface is derivatized to produce a stable charge excess, and then multi-layer films are built up on that surface by the electrostatic binding of alternatively charged layers of macromolecular compounds. This method has been applied to planar Au [6,7] and carbon electrodes [8], and also to colloidal suspensions of spherical particles of polystyrene latex [9–13]. The latter support material is attractive, as it provides an increase in the surface-to-volume ratio, and thus enables an increased amount of enzyme to be immobilized, relative to a planar surface. It has previously been applied to the LbL immobilization of the enzymes urease [9], glucose oxidase [10,11], horseradish peroxidase [11] and β-glucosidase [12], as well as the protein hemoglobin [13]. We are interested in the immobilization of polyphenol oxidase (PPO, also known as tyrosinase), for the construction of sensors for phenolic pollutants. The LbL immobilization of this enzyme has

* Corresponding authors. Tel.: +66 2 4709732; fax: +66 2 4523455.
E-mail addresses: werasak.sur@kmutt.ac.th (W. Surareungchai), s_mithran@yahoo.co.uk (M. Somasundrum).

0022-0728/$ - see front matter © 2006 Elsevier B.V. All rights reserved.
doi:10.1016/j.jelechem.2006.02.019

previously been demonstrated for planar electrodes of Au [7] and carbon [8].

In the LbL modification of latex, reports have consisted mainly of the synthesis of sub-micron spheres and the study of multi-layer enzyme deposition on them, monitored by either QCM [9,10] or zeta potential [9–11,13]. Although biosensors would seem to be one possible application for these biocolloids, extension to biosensing has so far only been examined in two cases, that of fluoresence-based glucose measurement using solution-phase spheres [10], and redox catalysis by hemoglobin-modified latex, adsorbed onto planar pyrolytic graphite [13]. The latter case was confined to CV studies of the redox catalysis of analytes such as O_2 and H_2O_2. Analysis of the sensor characteristics resulting from latex LbL-modification, in terms of sensitivity, rate determining steps etc., has not been performed.

In this paper, we wish to report the construction and kinetic analysis of cylindrical microelectrode sensors, consisting of single carbon fibres modified by PPO immobilized on latex (denoted Ty-La) by an LbL process. Our interest in using carbon fibre electrodes is that, in microelectrode terms, relatively large areas can be accessed (and therefore relatively large amounts of Ty-La adsorbed) by adjusting the fibre length, while still retaining the advantageous properties of radial diffusion [14]. To characterize the sensors, we have derived a general diffusion-kinetic model of the steady state current at PPO-modified microcylinders. Also, we have used latex particles of a micrometer scale, so that they can be viewed readily by optical microscope. Hence, modeling of the current may be combined with results from our previous optical characterizations of the physical and catalytic properties of colloidal suspensions of the Ty-La particles [15].

2. Experimental section

2.1. Reagents

Mushroom tyrosinase (EC 1.14.18.1) was purchased from Sigma. Poly(allylamine) hydrochloride (Aldrich) of mol. wt. 70 000 was dialyzed from water for 4 days using a dialysis membrane (Spectra/pro 132 680) with molecular cut off 12 000–14 000. All other chemicals were of reagent grade and used as received. The electrolyte for all electrochemical experiments was air-bubbled 0.1 M phosphate buffer, pH 6.8, containing 0.1 M KCl. All solutions were prepared using distilled water.

2.2. Preparation of tyrosinase-immobilized latex (Ty-La)

The details of both latex synthesis and tyrosinase immobilization are exactly as given previously [15]. The principle of the method, is that first the polystyrene spheres are coated with polystyrene sulphonate (PSS), to produce a negatively charged surface. The cationic poly(allylamine) (PAA) is then coated to leave a net positive charge, binding tyrosinase (isoelectric point = 4.7, therefore anionic at this pH), followed by a further PAA overlayer. Hence the spheres are envisaged as being coated by a single tyrosinase layer between two PAA layers.

2.3. Preparation of Ty-La carbon fibres

Carbon fibres of 3.5 μm radius were provided by Teijin Co., Japan. They were stored in absolute ethanol and dried thoroughly at room temperature before use. A single fibre was connected to a copper wire using silver-loaded epoxy, and then inserted into a glass tube and sealed with epoxy resin. To immobilize Ty-La, the fibre was placed in a Ty-La suspension for approx. 20 s, dipped in de-ionized water for a few minutes to wash off excess particles, and then dipped in a 0.02 mM solution of PSS in 0.5 M NaCl for 120 s. Following this, the fibres were again dipped in de-ionized water to remove weakly bound particles. This set of incubations was repeated 1–4 times as specified in Section 4.

2.4. Apparatus

Cyclic voltammetry data were collected on a HECS-112 potentiostat (Huso Electrochemical System). Amperometric experiments were performed using an Autolab 10 potentiostat (Eco Chemie). In both cases, the counter electrode was a Pt coil and potentials were set relative to a Ag|AgCl reference. Carbon fibres were viewed using an Olympus BX40 microscope. All experiments were performed at room temperature.

3. Theory

The current at planar tyrosinase enzyme electrodes has been modeled previously by Labbé and co-workers [8,16,17], but a model for cylindrical geometry has not so far been reported. We have considered this case as follows: we assume the micro-cylinder electrode to be coated uniformly by an enzyme immobilized in a non-conducting material which is porous to substrate. (The actual value of the porosity will affect the response in terms of partition coefficient and diffusion coefficient, as described in the derivation which follows.) The electrode is used in a stirred solution containing an excess of supporting electrolyte. The enzyme and electrode reactions are:

$$O_2 + 2\text{catechol} \rightarrow 2o\text{-quinone} + 2H_2O \quad (1)$$

$$o\text{-quinone} + 2H^+ + 2e^- \rightarrow \text{catechol} \quad (2)$$

Hence the catechol/quinone conversion forms an amplification cycle within the enzyme film. While it is possible in principle to solve for either phenol or catechol as substrate, solving for catechol is simpler, since it involves only one enzymic conversion. The actual mechanism of that conversion is complex, and involves three different states, oxy, met, deoxy [18] i.e. (where Ca is catechol, Q is quinone).

$$[\mathrm{Cu(I)–Cu(I)}]_{\mathrm{deoxy}} + \mathrm{O_2} + 2\mathrm{H_2O}$$
$$\xrightarrow{k_1}[\mathrm{H_2O–Cu(II)–O–O–Cu(II)–H_2O}]_{\mathrm{oxy}} \quad (3)$$
$$[\mathrm{H_2O–Cu(II)–O–O–Cu(II)–H_2O}]_{\mathrm{oxy}} + \mathrm{Ca}$$
$$\xrightarrow{k_2}[\mathrm{Cu(II)–Ca–Cu(II)}]_{\mathrm{met}} + 2\mathrm{H_2O} + 2\mathrm{H^+} \quad (4)$$
$$[\mathrm{Cu(II)–Ca–Cu(II)}]_{\mathrm{met}} \xrightarrow{k_3}[\mathrm{Cu(I)–Cu(I)}]_{\mathrm{deoxy}} + \mathrm{Q} \quad (5)$$

However, it has been shown that for monophenolic or *o*-diphenolic substrates, the process may be represented by Michaelis–Menten kinetics [19] i.e.

$$k_{\mathrm{cat}} = k_1 c_{\mathrm{O_2}} \quad (6)$$
$$K_{\mathrm{M}} = \frac{k_1(k_2+k_3)}{k_2 k_3} c_{\mathrm{O_2}} \quad (7)$$

Hence, in the following we have taken catechol as the analyte and have applied the low substrate approximation of the Michaelis–Menten equation, i.e. we have considered the sensor within its linear range. Therefore, in terms of radial distance, r, from the centre of the fibre, the mass balance for catechol at steady state can be written as

$$\frac{D_{\mathrm{C}}}{r}\frac{\mathrm{d}}{\mathrm{d}r}\left(r\frac{\mathrm{d}c_{\mathrm{C}}}{\mathrm{d}r}\right) - \frac{k_{\mathrm{cat}}c_{\mathrm{E}}c_{\mathrm{C}}}{K_{\mathrm{M}}} = 0 \quad (8)$$

where c_{I} is the concentration of species I (enzyme, catechol and quinone, respectively) and D_{I} is its diffusion coefficient. At steady state, the mass balance for *o*-quinone is

$$\frac{D_{\mathrm{Q}}}{r}\frac{\mathrm{d}}{\mathrm{d}r}\left(r\frac{\mathrm{d}c_{\mathrm{Q}}}{\mathrm{d}r}\right) + \frac{k_{\mathrm{cat}}c_{\mathrm{E}}c_{\mathrm{C}}}{K_{\mathrm{M}}} = 0 \quad (9)$$

For a diffusion-limited electrode reaction, assuming the solution is stirred strongly enough to disregard concentration gradients in bulk solution, the boundary conditions at the electrode surface (r_0) and the enzyme film surface (r_1) will be

$$r = r_0 : c_{\mathrm{Q}} = 0 \; c_{\mathrm{C}} = c_{\mathrm{C}}^* \quad (10)$$
$$r = r_1 : c_{\mathrm{Q}} = 0 \; c_{\mathrm{C}} = c_{\mathrm{C}}^* \quad (11)$$

where c_{C}^* is the bulk concentration of catechol scaled by the partition coefficient of the enzyme film. The steady state current can be obtained from

$$I/nF = 2\pi L r_0 D_{\mathrm{Q}}(\mathrm{d}c_{\mathrm{Q}}/\mathrm{d}r)_{r=r_0} \quad (12)$$

where $\mathrm{d}c_{\mathrm{Q}}/\mathrm{d}r$ can be determined from Eq. (9) once an expression for $c_{\mathrm{C}}(r)$ has been found. This may be done by integration of Eq. (8) under the boundary conditions, which gives

$$c_{\mathrm{C}}(r) = c_{\mathrm{C}}^* g[fI_0(\chi r) + K_0(\chi r)] \quad (13)$$

where $I_n(\chi r)$ and $K_n(\chi r)$ are modified Bessel functions of nth order, and

$$g = \frac{1}{fI_0(\chi r_0) + K_0(\chi r_0)} \quad (14)$$
$$f = \frac{K_0(\chi r_0) - K_0(\chi r_1)}{I_0(\chi r_1) - I_0(\chi r_0)} \quad (15)$$

and

$$\chi = \sqrt{\frac{k_{\mathrm{cat}}c_{\mathrm{E}}}{D_{\mathrm{C}}K_{\mathrm{M}}}} \quad (16)$$

The dimensionless concentration profile of catechol is shown in Fig. 1 for different values of χr_0. It can be seen that as the enzyme activity increases, the concentration of catechol falls at the centre of the film, but remains high at the film/solution interface, due to diffusion from bulk, and at the electrode/film interface due to generation at the electrode.

Substitution of Eq. (13) into Eq. (9) and integration under the boundary conditions, gives the concentration profile of *o*-quinone as

$$c_{\mathrm{Q}}(r) = \frac{D_{\mathrm{C}}c_{\mathrm{C}}^* g\chi}{D_{\mathrm{Q}}}\left\{-f\int_{r_0}^{r} I_1(\chi r)\mathrm{d}r + \int_{r_0}^{r} K_1(\chi r)\mathrm{d}r + \frac{\ln(r/r_0)}{\ln(r_1/r_0)}\left[f\int_{r_0}^{r_1} I_1(\chi r)\mathrm{d}r - \int_{r_0}^{r_1} K_1(\chi r)\mathrm{d}r\right]\right\} \quad (17)$$

As shown in Fig. 2, it is as expected the mirror image of the catechol profile, since one compound is being transformed into the other. Insertion of Eq. (17) into Eq. (12) then gives the dimensionless sensor response, j, as

$$j = \frac{I}{nFc_{\mathrm{C}}^* D_{\mathrm{C}} L} = 2\pi\chi g \times \left\{r_0[-fI_1(\chi r_0) + K_1(\chi r_0)] + \frac{1}{\ln(r_1/r_0)}\left[f\int_{r_0}^{r_1} I_1(\chi r)\mathrm{d}r - \int_{r_0}^{r_1} K_1(\chi r)\mathrm{d}r\right]\right\} \quad (18)$$

This expression may be simplified by considering limiting cases and approximating the values of the Bessel functions accordingly. When χr_0 and χr_1 are so large that $I_n(x) \approx \mathrm{e}^x/(2\pi x)^{1/2}$ and $K_n \approx \mathrm{e}^{-x}(\pi/2x)^{1/2}$, Eq. (18) is reduced to

$$\frac{I}{nF} = 2\pi r_0 L c_{\mathrm{C}}^* D_{\mathrm{C}}\chi \quad (19)$$

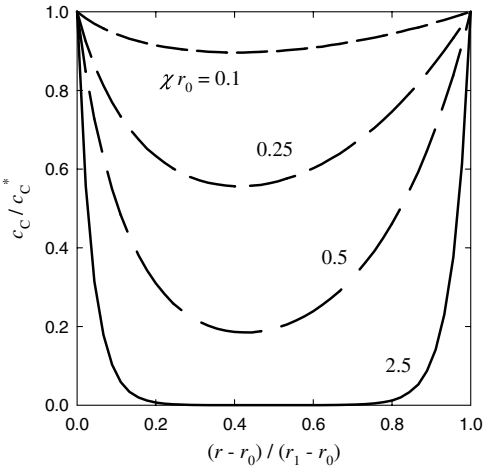

Fig. 1. Normalized concentration profile of catechol, plotted from Eq. (13) for different ratios of enzyme activity: substrate diffusion (see text for definitions).

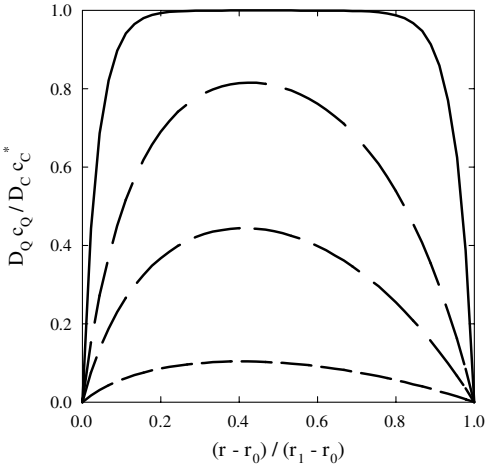

Fig. 2. Normalized concentration profile of *o*-quinone, plotted from Eq. (17) for different ratios of enzyme activity:substrate diffusion (see text for definitions).

While if χr_0 and χr_1 are small enough for the Bessel functions to be approximated as: $I_0 \approx 1$, $I_1(x) \approx x/2$, $K_0(x) \approx -\ln(x)$, $K_1(x) \approx 1/x$, then Eq. (18) becomes

$$\frac{I}{nF} = \frac{\pi c_C^* L k_{cat} c_E}{K_M}\left[\frac{r_1^2 - r_0^2}{2\ln(r_1/r_0)} - r_0^2\right] \quad (20)$$

Hence, in varying the thickness of the enzyme layer, we may expect the current to first increase and then to become thickness-independent. This transition is shown in Fig. 3, where the dimensionless response is plotted from Eq. (18) as a function of dimensionless film thickness for different values of χr_0. The main difference between the characteristics here and those of an oxidase-based micro-cylinder system [20], is that the response here does not become limited by diffusion through the film at high values of χr_0, but remains partly controlled by enzyme kinetics. This is due to the substrate recycling effect of the electrode. Obviously, in practice the response will not increase forever with

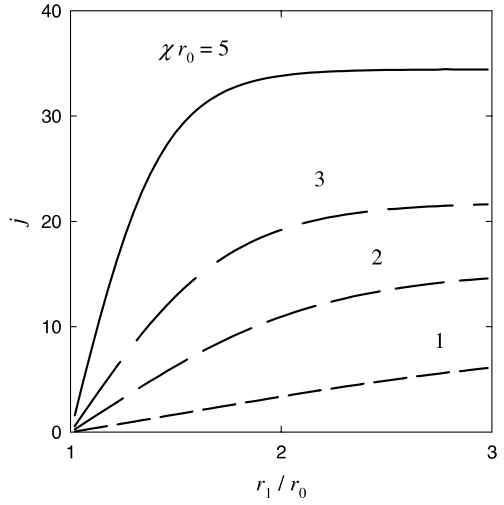

Fig. 3. Dimensionless sensor response as a function of dimensionless film thickness, plotted from Eq. (18) for different ratios of enzyme activity: substrate diffusion.

enzyme activity, but instead at very high activity, the rate determining step will be diffusion of substrate through the Nernst diffusion layer.

It can be noted that Eq. (19) is essentially the same as the planar electrode expression derived by Desprez and Labbé [16] for high values of χ. This is because at high values of χ, the catechol entering from bulk will react close to the film-solution interface, and so the *o*-quinone will be generated here. This can be seen from the concentration profiles for catechol and *o*-quinone shown in Figs. 1 and 2, respectively. It can be observed that at high values of χr_0 the normalised concentrations of catechol and *o*-quinone through the central region of the film will approach 0.0 and 1.0, respectively. Hence, the effect of radial diffusion is negligable and the resulting concentration profiles take the symmetrical shape previously demonstrated by Desprez and Labbe for the planar case [16]. In contrast, at low values of χr_0 the profiles of catechol and *o*-quinone become asymmetric, with the respective minima (catechol) and maxima (*o*-quinone) shifting closer to the electrode surface. This occurs because the enzyme substrate now permeates the whole film before reacting. Thus, *o*-quinone is generated through the film and diffuses to either the electrode surface, where it reacts, or the film surface, where it is lost to bulk. For a steady state to exist, the rate of material consumed at each interface (i.e. in mol s^{-1}) must be the same. Since the consuming area at the electrode ($2\pi r_0 L$) is less than the area of the outer edge of the film ($2\pi r_1 L$), to achieve an equal rate of consumption the flux to the electrode must be greater than the flux to the solution, to compensate. Therefore the concentration gradient is steeper in the direction of the electrode. This behaviour has been observed for the same reason in the modeling of H_2O_2 generation by oxidase enzymes assuming hemispherical diffusion [21]. Thus, in the low χ case described by Eq. (20), the resulting expression is different from the planar equation [16].

An alternative way to treat Eq. (18) is to search for a simpler semi-empirical equation which may replace it. We have obtained the expression

$$j = 2\pi x^q \tanh[(x/2)(\alpha - 1)^p] \quad (21)$$

which relates the dimensionless response to the dimensionless parameters $x(=\chi r_0)$ for enzyme kinetics and $\alpha(=r_1/r_0)$ for film thickness. For values of $x > 9.5$, Eq. (21) may replace Eq. (18) with less than 5% error. For some lower values of x, Eq. (21) may be fitted to Eq. (18) by altering the values of p and q, as given in Table 1. Note that the above

Table 1
Values of p and q which fit Eq. (21) to Eq. (18) with <5% error

x	p	q
9.0–7.0	1.00	1.01
6.0–4.0	1.03	1.05
3.0	1.04	1.10
2.0	1.02	1.14[a]/1.25[b]

[a] Valid for $\alpha \leqslant 2.0$.
[b] Valid for $\alpha > 2.0$.

treatment is not restricted to latex-modified microcylinders, but is suitable for any PPO coating of a microcylinder that satisfies the previously stated film and boundary conditions.

4. Results and discussion

4.1. Pretreatment of carbon fibre

It is known that the pretreatment of carbon fibres by electrochemical or chemical means can change their surface properties, and thus, the electrochemical and adsorptive properties of compounds which react at them [22]. Therefore, we examined the effect of pretreatment on the electrochemistry of both catechol and the Ty-La particles. The effect of a 'weak' (cycled 20 times between −0.2 V and 2.0 V at 1.0 V s^{-1}) and a 'stronger' pretreatment (cycled 10 times between −0.2 V and 2.5 V at 1.0 V s^{-1}) were compared with that of no pretreatment. In Fig. 4 cyclic voltammograms (50 mV s^{-1} sweep rate) are shown of 0.45 mM catechol in phosphate buffer, pH 6.8, at each type of fibre. It can be seen that without pretreatment (curve (a)) catechol is not electroactive, where as both methods of pretreatment result in electroactivity. It has been shown that electrochemical pretreatment of carbon cleans the surface [23,24], and also that cleaning procedures at bulk carbon electrodes improve the catechol/*o*-quinone redox system [25]. This was thought to be because cleaning facilitated adsorption prior to electron transfer, and that adsorption lowers the large inner-sphere reorganisation energy that is required in catechol/*o*-quinone conversion due to significant bond length changes in the reaction. The 'weaker' pretreatment method (curve (b)), produces a greater double layer current and peaks for the oxidation of catechol and reduction of the quinone. In comparison, the 'stronger' pretreatment method (curve (c)) results in a sigmoidal voltammogram of lower limiting currents than the 'weak' pretreatment. It has been reported that very strong pretreatments of carbon fibre produce an insulating layer of graphite oxides [26]. Hence, it is likely that curve (c) is recorded at a partially insulated surface, in which cracks in the oxide layer provide the actual reaction area. Hence there is lower current and a greater effect of radial diffusion.

Fig. 5 (A to C) shows voltammograms for each type of fibre (50 mV s^{-1} scan rate) following the adsorption of Ty-La particles. Curve (a) of each voltammogram set, is a scan of a Ty-La-modified fibre in the absence of catechol. It can be seen that the Ty-La particles themselves are not electroactive at any of the fibres. Curves (b) and (c) of each set, represent 0.45 mM catechol at a Ty-La fibre and at an enzyme-free fibre, respectively. At the unmodified carbon fibre (A), no clear catalytic effect can be observed, due to slow kinetics of catechol at this surface. At the modified fibres (B & C), an increase in the negative current peak (weak pretreatment) and limiting value in sigmoid (strong pretreatment), indicates the cycling effect of the enzyme

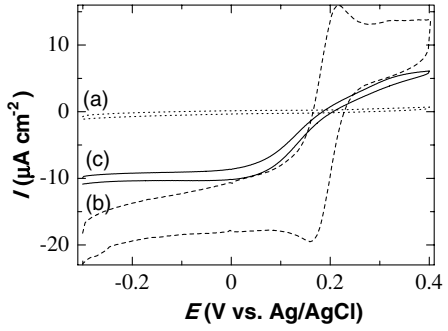

Fig. 4. Cyclic voltammograms at 50 mV s^{-1} of 0.45 mM catechol at untreated (a), 'weakly' pretreated (b), and 'strongly' pretreated (c) carbon fibre electrodes. Electrolyte is air-saturated 0.1 M phosphate buffer, pH 6.8 containing 0.1 M KCl.

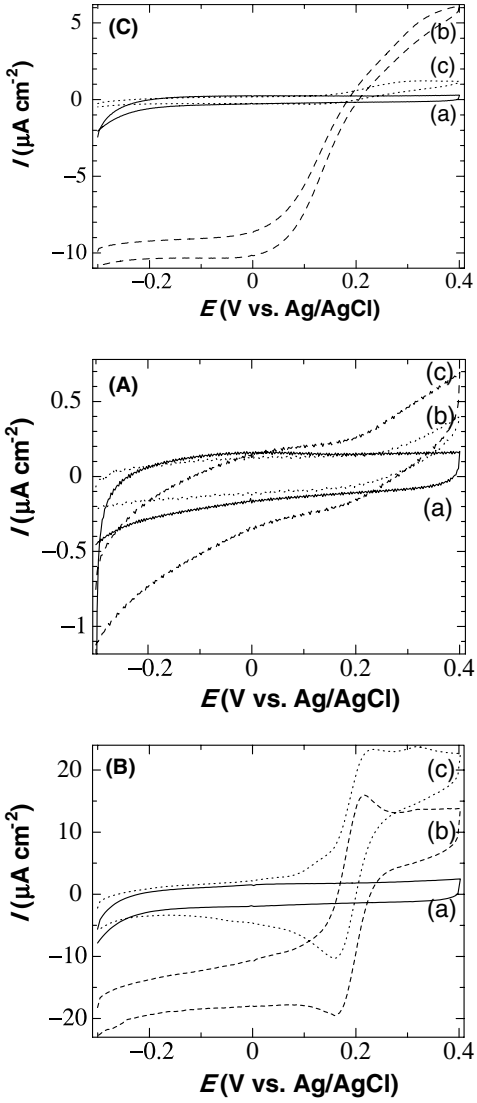

Fig. 5. Cyclic voltammograms at 50 mV s^{-1} of untreated (A), 'weakly' pretreated (B), and 'strongly' pretreated (C) carbon fibre electrodes. Each voltammogram set shows a Ty-La modified electrode in the absence (a) and presence (b) of 0.45 mM catechol, and an enzyme-free electrode in the presence of 0.45 mM catechol (c). Electrolyte as in Fig. 4.

increasing the concentration of *o*-quinone at the electrode. We viewed the Ty-La fibres by optical microscope before and after voltammetry, as shown in Fig. 6. The Ty-La particles were initially closely packed. However, after voltammetry there was a noticeable loss of Ty-La particles from the unmodified fibre, while the other two fibres appeared essentially the same. Hence, the effect of pretreatment has been to both improve the electrochemistry of catechol and the adsorptive properties of the carbon fibre for Ty-La.

The amperometric steady state current for catechol was calibrated at −100 mV at each type of fibre, after Ty-La adsorption. The results, shown in Fig. 7, indicate that the 'weak' pretreatment method produced the highest response. The response time for a steady state current at this fibre for low (e.g. 1.7 μM) to high (e.g. 16.6 μM) catechol concentrations varried from 12 s to 44 s, respectively. Since microscope observation does not indicate differences in the amount of Ty-La adsorbed by either method, the main reason for the higher response is likely to be due to the lower active electrode area at the strongly pretreated fibre, due to graphite oxides.

4.2. Kinetics of Ty-La-coated carbon fibres

Sensors constructed by the 'weak' pretreatment method were studied further. The effect of enzyme layer thickness was examined by performing repeated incubations in Ty-La suspension, to increase the amount of Ty-La adsorbed. Fig. 8 shows calibrations to catechol using fibres prepared by 1–4 incubations. It can be seen that the response increases from 1 to 2 incubations and is essentially constant from 2 to 3. However, in contradiction to the theory, going from 3 to 4 incubations, the response is lower. This is probably because the path to the electrode, i.e. the spaces admitting solution between the closely packed Ty-La particles, becomes significantly more tortuous at a high Ty-La loading, and therefore the effective diffusion coefficient becomes smaller [27]. Since the sensitivity from 2 and 3 incubations is effectively thickness independent, we may apply Eq. (19) to the linear range of this data. Hence, the square of the gradient of the solid line in Fig. 8 is equal to the parameter $\kappa^2 D_C k_{cat} \gamma c_E^T / K_M$, where κ is the partition coefficient of the film to catechol and the concentration of active enzyme,

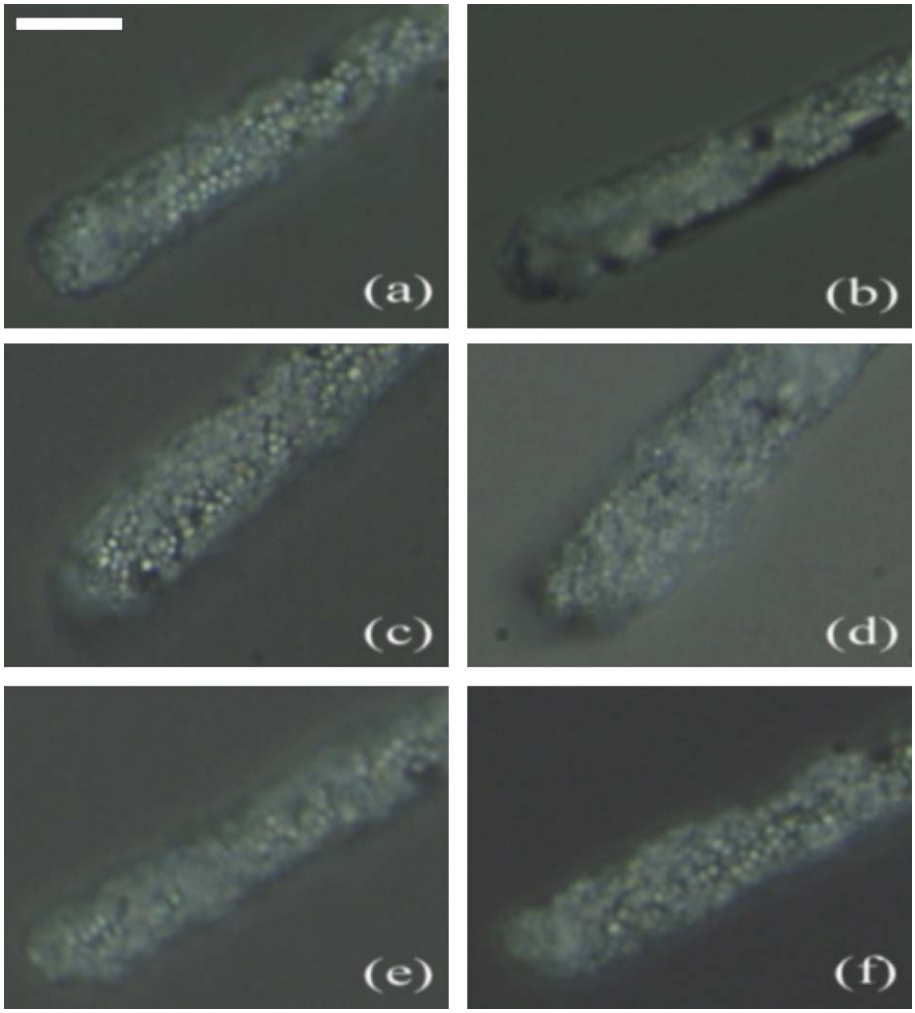

Fig. 6. Optical microscope photographs of carbon fibre electrodes modified by Ty-La particles before ((a) untreated, (c) weakly pretreated, (e) strongly pretreated) and after ((b) untreated, (d) weakly pretreated, (f) strongly pretreated) recording the voltammograms shown in Fig. 5. Scale bar in top left hand corner is 10 μm.

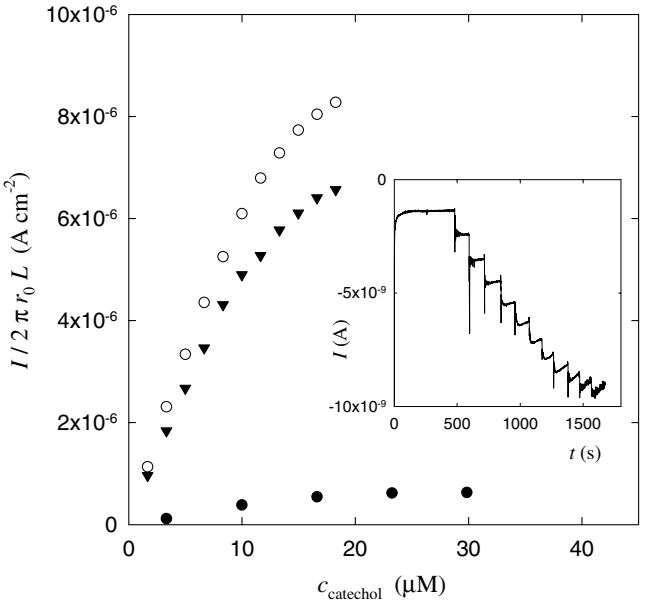

Fig. 7. Amperometric calibration at −100 mV using untreated (●), 'weakly' pretreated (○), and 'strongly' pretreated (▼) carbon fibre electrode modified by single incubation in Ty-La suspension. Electrolyte as in Fig. 4. Inset shows current-time curve used for (○).

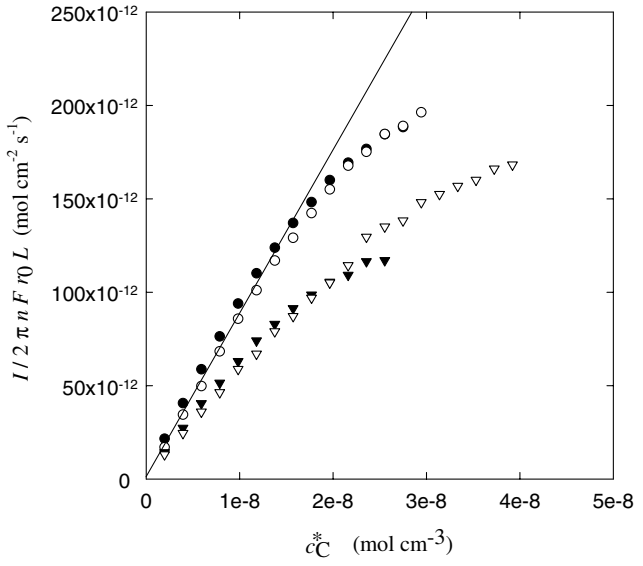

Fig. 8. Amperometric calibration of catechol at −100 mV using 'weakly' pretreated carbon fibre electrode modified by 1 (▼), 2 (●), 3 (○), or 4 (▽) incubations in Ty-La suspension. Electrolyte as in Fig. 4. Solid line is best fit of linear range to Eq. (19).

c_E^A, is related to the total enzyme concentration, c_E^T, by $c_E^A = \gamma c_E^T$.

In the case of the 1 incubation fibre, as the sensitivity increases with film thickness, the data may possibly fit Eq. (20), provided the electrode is functioning in the purely kinetic domain treated by this limiting case. To examine this, we produced single incubation fibres containing a reduced concentration of tyrosinase. This was done by preparing mixtures of Ty-La and PAA-coated tyrosinase-free latex at varying known ratios. Hence, the amount of tyrosinase transferred to the fibre was diluted. We note that for both types of latex, a PAA layer is outermost, and therefore both types should have the same adsorption characteristics. Therefore we have assumed the Ty-La:Ty-free ratio in the suspension is the same as that on the electrode. Catechol was measured at each fibre, and the length and diameter of the fibre then measured by optical microscope. The quantity of tyrosinase on the spheres was calculated from optical measurements of a sample of Ty-La spheres. After the first coating of PAA, the spheres had a mean diameter of 1.73 μm with a standard deviation, σ, of 0.14 μm for $n = 177$ spheres measured. Hence, assuming a normal distribution, 99.9% of the diameters were within the range 1.73 ± 0.035 μm [28], i.e. 1.73 μm ± 2.0%. After the tyrosinase coating, a sample of spheres had a mean diameter of 1.75 μm ($\sigma = 0.15$, $n = 155$). Therefore 99.9% of these were within the range 1.75 ± 0.039 μm, i.e. 1.75 μm ± 2.2%. Clearly, the difference between the mean diameters includes ambiguity, since it is less than the standard deviation. The mean volume of tyrosinase immobilised is $(4\pi/3)(r_{PPO}^3 - r_{PAA}^3)$. Assuming a density of unity, this corresponded to a mass of 9×10^{-14} g ± 12.6%, (since in performing the calculation the percentage errors are multiplied by three and then summed). This is 7×10^{-19} moles ± 12.6% based on a relative molecular mass of 1.28×10^5 g mol^{-1} [7,29]. The concentration of enzyme in the latex layer was then estimated by calculating the number of Ty-La spheres in a given cross-section of the coated fibre, equal to $(r_1^2 - r_0^2)/r_{Ty-La}^2$, and multiplying this by the number of Ty-La-wide cross-sections along the length of the fibre, equal to $L/d_{Ty\text{-}La}$ (where $r_{Ty\text{-}La}$ is the radius of a Ty-La sphere and d is its diameter, found to be 1.77 μm ± 2.0%, $\sigma = 0.15$ μm, $n = 187$). Thus we may calculate the total number of moles of tyrosinase contained in a film of volume $\pi L(r_1^2 - r_0^2)$. For the diameter of the Ty-La-coated fibre, an average value was used after observation at different points along its length. Typically 3 - 9 measurements were taken, depending on the lack of uniformity of the Ty-La coating. There was a variation of up to ±2 μm for a given fibre. Hence, this represented the greatest source of error in the estimation of the enzyme concentration and was from ±19% to ±21% for the fibres examined. Since the calculations use the values of r_1^2, there is an overall error of ±40% from these measurements.

Amperometric measurements were performed using the fibres prepared with diluted Ty-La, and the fit of the resulting sensitivities to Eq. (20) is given in Fig. 9. There is notable scatter in this plot, which is no doubt due to the Ty-La coated fibres not being of fully uniform diameter.

From Eqs. (19) and (20), the square of the gradient of the solid line in Fig. 8 divided by the gradient of the solid line in Fig. 9, is equal to $\kappa D_C c_E^T$ and has a value of 1.88×10^{-13} mol cm^{-1} s^{-1}. It should be noted that the determination of this parameter marks an advantage of micro-cylinders over planar electrodes for the kinetic analysis of PPO-biosensors, as in contrast, the planar

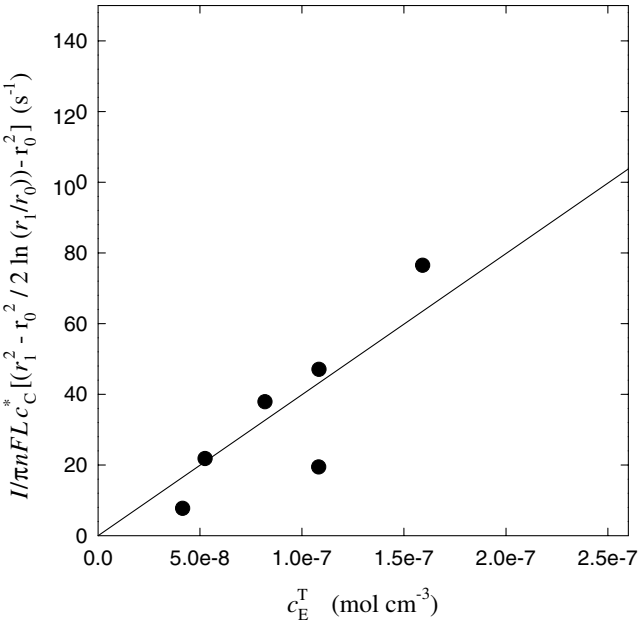

Fig. 9. Sensitivities of amperometric calibrations to catechol (−100 mV), using fibres modified by incubation in diluted Ty-La suspensions. Electrolyte as in Fig. 4. Enzyme concentrations calculated from optical measurements as described in text. Solid line is best fit to Eq. (20).

expressions analogous to Eqs. (19) and (20) do not allow the terms L, K_M, γ and k_{cat} to be eliminated [16].

The mean value of c_E^T for the fibres coated by 1 to 3 incubations in un-diluted Ty-La was $1.60 \times 10^{-7} \pm 0.02 \times 10^{-7}$ mol cm^{-3}. Noting there is a ± 40% error in the determination of each concentration, this gives a mean c_E^T of 1.6×10^{-7} mol cm^{-3} ± 41%. Therefore κD_C is estimated as 1×10^{-6} cm^2 s^{-1} ± 41%. Even providing for the experimental error, this is still only around one order of magnitude lower than the solution value (1.8×10^{-5} cm^2 s^{-1} [8]). This is reasonable, given that the thickness of each layer of Tyr or PAA was measured at <0.03 μm. Since the enzyme and outer layer are so thin, we expect the resultant diffusion coefficient to predominantly represent movement through solution channels between the latex spheres. Given this, it seems acceptable to assume a partition coefficient of unity for this system. Thus, we may calculate the kinetic length ($1/\chi$) to be 1.4×10^{-4} cm, which is in good agreement with optical measurement of the Ty-La film thicknesses. These were 1.5×10^{-4} cm, 3.7×10^{-4} cm and 1.8×10^{-3} cm for 1, 2 and 3 incubations respectively. Hence the proportion of film in which the catechol was consumed by tyrosinase, decreased from approximately 93% to 37% to 18% on increasing the film thickness with successive incubations. This agrees with the theoretical prediction that the response should become thickness-independent once reaction is localized at the outer layers of the latex film. (Note that we are refering here to the catechol diffusing from bulk. Catechol will also react at the latex inner layers, having been regenerated by the electrode as indicated in the concentration profile in Fig. 1).

Returning to Fig. 9, the gradient of this plot is equal to $\gamma k_{cat}/K_M$ and has a value of 4.0×10^8 mol^{-1} cm^3 s^{-1} ± 40% (since the error in this determination is the error in c_E^T). We previously performed spectrophotometric measurements of a homogeneous suspension of a known quantity of Ty-La particles [15], from which a Hanes-Wolf plot gave K_M for the immobilised tyrosinase as 0.15 mM. Using this value, γk_{cat} is equal to 60 s^{-1} ± 40%. This is of the same order of magnitude as the value calculated from the Hanes-Wolf plot itself (49 s^{-1}), which suggests the conclusions of the kinetic analysis are reasonable. A Hanes-Wolf plot for the free enzyme [15] gave $K_M = 0.92$ mM and $k_{cat} = 2381$ s^{-1}. The value of γ will depend on whether k_{cat} has altered. Since we would not generally expect an *increase* in k_{cat} on immobilisation, one interpretation of the data is that the minimum proportion of active enzyme is approx. 2–3% of that immobilised.

4.3. Analytical use of Ty-La carbon fibres

A Ty-La fibre coated by 2 incubations was used to calibrate phenol and the result is shown in Fig. 10. Compared to catechol detection using the same coating, the sensitivity for phenol was less (1.5 nA μM^{-1} mm^{-2} cf. 17.2 nA μM^{-1} mm^{-2} for catechol) and the linear range was longer (7–56.5 μM cf. 2–19.7 μM for catechol), both of which are consistent with the solution phase comparisons of tyrosinase for these substrates [8].

As shown in Fig. 11, the response to catechol decreased with repeated assays; the rate of decrease being approximately the same for assays at both 0.38 mM and 1.97 μM. This suggests the limiting stability factor was desorption of the latex, rather than passivation during

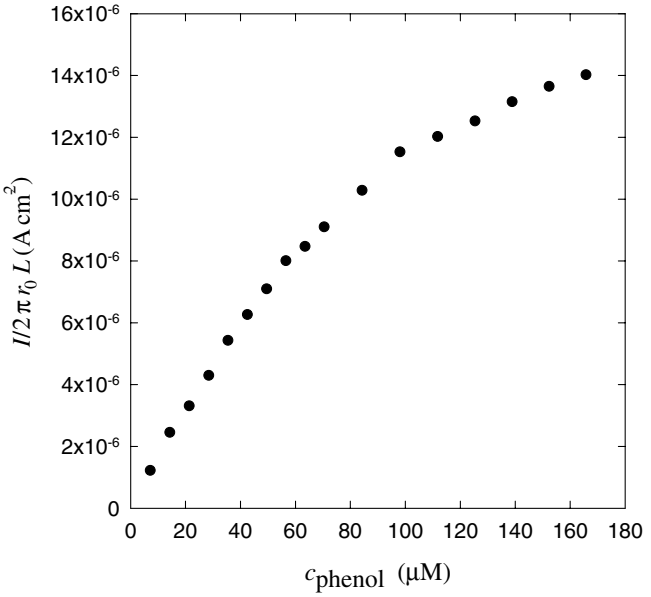

Fig. 10. Amperometric calibration of phenol at −100 mV, using carbon fibre electrode modified by 2 incubations in Ty-La suspension. Electrolyte as in Fig. 4.

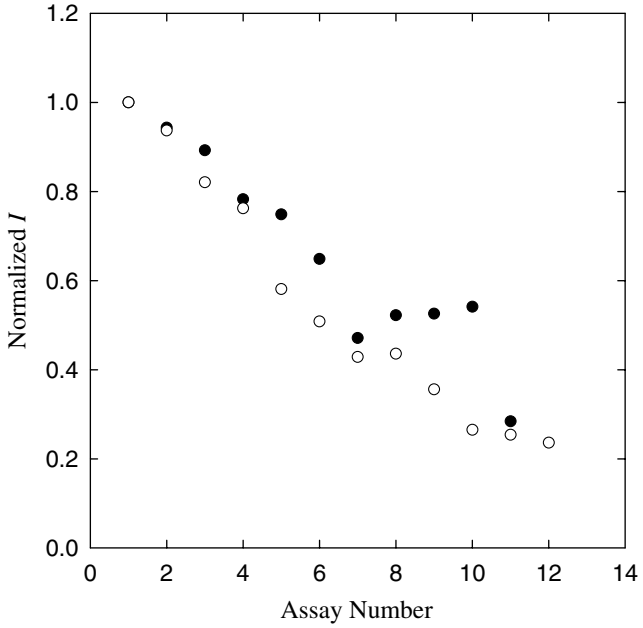

Fig. 11. Repeated amperometric response to catechol (−100 mV) at 0.38 mM (●) and 1.97 μM (○), each at a single fibre modified by 2 incubations in Ty-La suspension. Electrolyte as in Fig. 4.

o-quinone electro-reduction, since if passivation was occuring, we would expect the extent to increase with increased concentration of *o*-quinone at the electrode. This interpretation was also suggested by repeated cyclic voltammetry of catechol at a weakly pretreated fibre, as shown in Fig. 12, where after an initial decrease within the first five scans, the cathodic peak height remained stable for the next 15 scans, suggesting the catechol/quinone couple was reacting without electrode fouling.

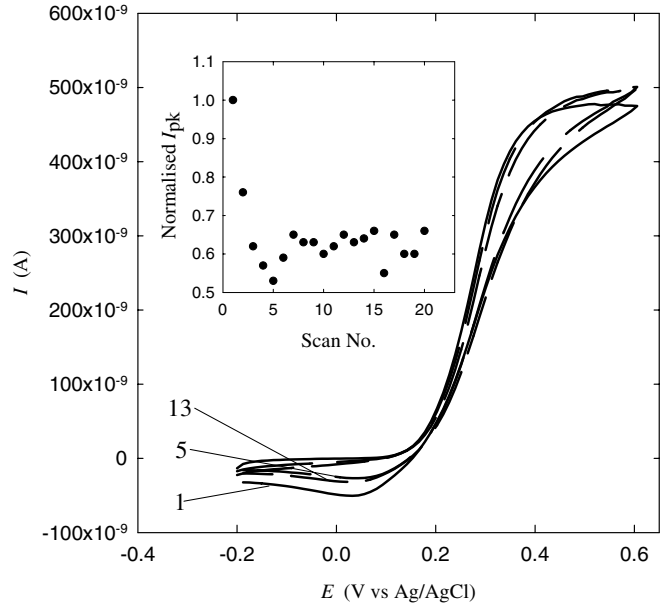

Fig. 12. Repetitive cyclic voltammograms of 0.45 mM catechol using a 'weakly' pretreated carbon fibre. First, 5th and 13th scans shown. Scan rate is 50 mV s^{-1}. Inset shows change in cathodic peak height with scan number. Electrolyte as in Fig. 4.

5. Conclusions

Carbon fibres modified by PPO-labelled latex spheres have been shown to be responsive to phenol and catechol. Characterisation of the spheres was facilitated by the fact that they were of a size readily viewable by optical microscope. The catechol responses could be described by approximate analytical solutions to a diffusion-kinetic model, provided the amount of latex adsorbed was not so high that the effective diffusion coefficient of catechol decreased across the examined range.

As predicted by the model, for a given enzyme concentration, the substrate response became thickness independent once the thickness increased significantly beyond the kinetic length of the substrate. Application of the model to experimental data revealed that at minimum 2–3% of the immobilized enzyme was catalytically active, and also indicated that this form of modification provided a relatively open film structure, in which substrate diffusion probably consisted predominantly of movement through solution channels between adjoining latex spheres. However, it should be noted that in these experiments the spheres were coated by only one layer of tyrosinase, with a thin outer layer of PAA. If very many tyrosinase/PAA layers are built up, we may expect the effective diffusion coefficient to eventually increase, as transport through the actual enzyme layers becomes a significant barrier.

Although the adsorption of latex particles here was significantly better than our previous reports using planar Pt electrodes [15], latex desorption was still the limiting factor in sensor stability. It may be possible to increase long term adsorption by other methods of fibre pretreatment, and this is currently being examined.

Acknowledgements

P.R. was supported by the Fukui University Student Exchange Program (FUSEP) in Japan and a Ph.D. studentship from the National Center for Genetic Engineering and Biotechnology (BIOTEC), in Thailand. The research was also supported by Grants-in-Aid for Scientific Research (Grant 14340232) in Japan. M.S. is an employee of BIOTEC.

References

[1] G. Decher, H.D. Hong, Ber. Bunsen-Ges. Phys. Chem. 95 (1991) 1430.
[2] G. Decher, Science 277 (1991) 1232.
[3] Y. Lvov, F. Essler, G. Decher, J. Phys. Chem. 97 (1993) 13773.
[4] Y. Lvov, G. Decher, H. Mohwald, Langmuir 9 (1993) 481.
[5] Y. Lvov, G. Decher, G. Sukhorukov, Macromolecules 26 (1993) 5396.
[6] J. Hodak, R. Etchenique, E.J. Calvo, K. Singhal, P.N. Bartlett, Lamgmuir 13 (1997) 2708.

[7] E.S. Forzani, V.M. Solis, E.J. Calvo, Anal. Chem. 72 (2000) 5300.
[8] L. Coche-Guerante, P. Labbé, V. Mengeand, Anal. Chem. 73 (2001) 3206.
[9] Y. Lvov, F. Caruso, Anal. Chem. 73 (2001) 4212.
[10] M. Fang, P.S. Grant, M.J. McShane, G.B. Sukhorukov, V.O. Golub, Y. Lvov, Langmuir 18 (2002) 6338.
[11] F. Caruso, C. Schuler, Langmuir 16 (2000) 9595.
[12] F. Caruso, H. Fiedler, K. Haage, Colloids Surf., A: Physiochem. Eng. Aspects 169 (2000) 287.
[13] H. Sun, N. Hu, Biophys. Chem. 110 (2004) 297.
[14] S.T. Singelton, J.J. O'Dea, J. Osteryoung, Anal. Chem. 61 (1989) 1211.
[15] P. Rijiravanich, K. Aoki, J. Chen, W. Surareungchai, M. Somasundrum, Electroanalysis 16 (2004) 605.
[16] V. Desprez, P. Labbé, J. Electroanal. Chem. 415 (1996) 191.
[17] L. Coche-Guerente, V. Desprez, J.-P. Diard, P. Labbé, J. Electroanal. Chem. 470 (1999) 53.
[18] D.E. Wilcox, A.G. Porras, Y.T. Hwang, K. Lerch, M.E. Winkler, E.I. Solomon, J. Am. Chem. Soc. 107 (1985) 4015.
[19] J. Carbanes, F. Garcia-Canovas, J.A. Lozano, F. Garcia-Carmona, Biochim. Biophys. Acta 923 (1987) 187.
[20] M. Somasundrum, K. Aoki, J. Electroanal. Chem. 530 (2002) 40.
[21] C. Phanthong, M. Somasundrum, J. Electroanal. Chem. 558 (2003) 1.
[22] R.L. McCreery, in: P.T. Kissinger, W.R. Heineman (Eds.), Laboratory Techniques in Electroanalytical Chemistry, Marcel Dekker Inc., New York, 1996, p. 986.
[23] R.C. Engstrom, Anal. Chem. 54 (1982) 2310.
[24] C.D. Allred, R.L. McCreery, Anal. Chem. 64 (1992) 444.
[25] S.H. DuVall, R.L. McCreery, Anal. Chem. 71 (1999) 4594.
[26] P.M. Kovach, M.R. Deakin, R.M. Wightman, J. Phys. Chem. 90 (1986) 4612.
[27] E.J. Bailey, F.D. Ollis, in: Biochemical Engineering Fundamentals, 2nd Ed., McGraw-Hill, New York, 1986, p. 458.
[28] A. Jeffrey, Mathematics for Engineers and Scientists, fourth ed., Chapman & Hall, 1989, p. 828.
[29] J.P. Gillespie, Comp. Biochem. Physiol. 98C (1991) 351.